Adsorption of Thiophene on the RuS_2 (100) and (111) Surfaces: A Laplacian of the Electronic Charge Density Study

Yosslen Aray,*,†,‡ Jesus Rodríguez,† David Vega,§ Santiago Coll,†,|| Eloy Nouel Rodríguez-Arias,|| and Felix Rosillo⊥

Centro de Quimica, IVIC, Apartado 21827, Caracas 1020 A, Venezuela, Physical and Chemical Properties Division, National Institute of Standards and Technologies, NIST, Gaithersburg, Maryland 20899, FACYT, Universidad de Carabobo, Valencia, Venezuela, Laboratorio de Modelaje de Catálisis, Departamento de Química, Universidad Simón Bolivar, Caracas, Venezuela, and Facultad Experimental de Ciencias, Departamento de Química, Universidad del Zulia, Maracaibo, Venezuela

Received: July 22, 2002; In Final Form: October 16, 2002

To study the effect of the surface Ru sulfur coordination number and of the surface S−H and Ru−H species into the thiophene adsorption on RuS_2, a topologic study of the Laplacian of the electronic density of selected (100) and (111) surfaces was carried out. It was found that a nonbonded local charge concentration on the S atom of the thiophene interacts with a local minimum on the outermost Ru atoms of the surfaces. This interaction is strongly affected by a nonbonded local charge concentration located on the outermost S atoms of the surface. Both interactions combine in such way that the strength of the thiophene adsorption on the unhydrogenated surfaces shows small changes. The main role of the S−H bond is to move away the surface sulfur local charge concentrations from the Ru atoms while the Ru−H species favors the hydride attacks to a local minimum located at the C_α of the thiophene molecule.

Introduction

Transition metal sulfides (TMS) belong to a very important class of catalysts characterized by being stable under strong conditions in sulfo-reductive hydroprocessing of petroleum-based feedstocks.[1,2] In hydrodesulfurization (HDS) processes, organosulfur molecules are removed from oil by reacting with hydrogen to form H_2S and hydrocarbons.[1−3] The catalytic process of sulfur removal involves both a C−S bond cleavage and a hydrogenation step. Studies of HDS of dibenzothiophene (DBT) over unsupported sulfides[4] showed that the ability of a particular sulfide to catalyze the HDS reaction is related to the position of the TM in the periodic table. A characteristic volcano type dependence of the activity of the metal as a function of its position in the periodic table, for second (4d) and third row (5d) transition metals, was found. A maximum is attained for RuS_2, which is one of the most active TMS. Several theoretical[5−20] studies have been carried out in order to explain the behavior discussed above. In a recent paper,[18] it was shown that all of the experimental HDS[4] activities of the TMS, A_{TMS}, fit on a single volcano master curve when plotted against the bulk TM−S bond strength, defined as the bulk cohesive energy per metal−sulfur bond. This correlation was corroborated[20] by means of a bond concept rigorously defined in the context of the topological theory of the electronic density, $\rho(\mathbf{r})$. A topological analysis[21] of the Laplacian of the electronic charge density, $L(\mathbf{r}) = -\nabla^2\rho(\mathbf{r})$ of bulk 4d TMS suggested that such a volcano plot is a consequence of the quite different nature of the TM−S interactions for layered and isotropic TMS. However, catalysis is largely a surface event and the degree of coordinative unsaturation of the metal atoms on the surfaces may play an important role in the HDS catalysis[22] and the sulfur coordination may be very different from the bulk situation. In fact, anion vacancies on surface/edges of the catalyst are considered the actives sites for HDS. Hydrogen achieves an important role in this aspect, removing sulfur from the surface and creating vacancies around the metals.[3] Two types of hydrogen species have been experimentally[23] characterized on the RuS_2 surface: protonlike SH and hydridelike Ru−H. A recent quantum chemistry density functional theory (DFT) study[24] of thiophene (TP) adsorption over different hydrogenated RuS_2 (111) defect surface termination has shown that the presence of Ru−H favors the TP activation. In the present work, to explore the effect of the Ru sulfur coordination number (SCN) into the TP adsorption on RuS_2, we have carried out a systematic determination of the topology of $L(\mathbf{r})$ of selected (100) and (111) surfaces. These are the two surfaces most frequently exposed by RuS_2 crystals. In addition, we also study the $L(\mathbf{r})$ topology of the hydrogenated (111) RuS_2 surface in order to explore the effect of the S−H and Ru−H species.

Surface Models

Ruthenium disulfide bulk is a pyrite type crystal whose lattice[25] is described by the cubic space group *Pa*3 with cube edge length $a = 5.611$ Å. Its structure can be described as a face-centered cube (fcc) of Ru atoms (see Figure 1a) with pairs of S_2 molecules located (see Figure 1b) in the middle of the cube edges and at the cube center. Each Ru atom is bonded to six molecules (SCN = 6) in an octahedral arrangement. Each S atom has three Ru neighbors so a S_2 pair is bonded to six metal neighbors in a pseudo-octahedral coordination. There is only one type of S−S and Ru−S bond in this structure.

* To whom correspondence should be addressed. Fax: (+58)212 504 1350. E-mail: yaray@ivic.ve.
† IVIC.
‡ National Institute of Standards and Technologies.
§ Universidad de Carabobo.
|| Universidad Simón Bolivar.
⊥ Universidad del Zulia.

10.1021/jp021692b CCC: $22.00
Published on Web 11/21/2002

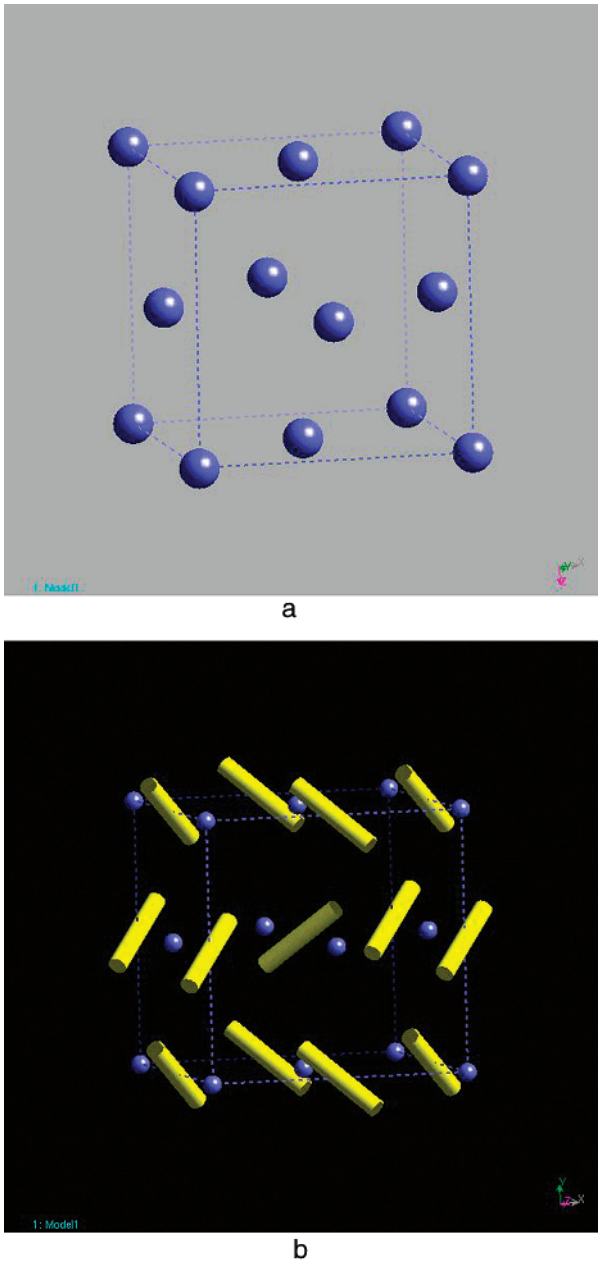

Figure 1. 3D view of RuS_2 illustrating (a) the fcc arrangement of Ru atoms (blue spheres) and (b) S2 pairs (yellow cylinders).

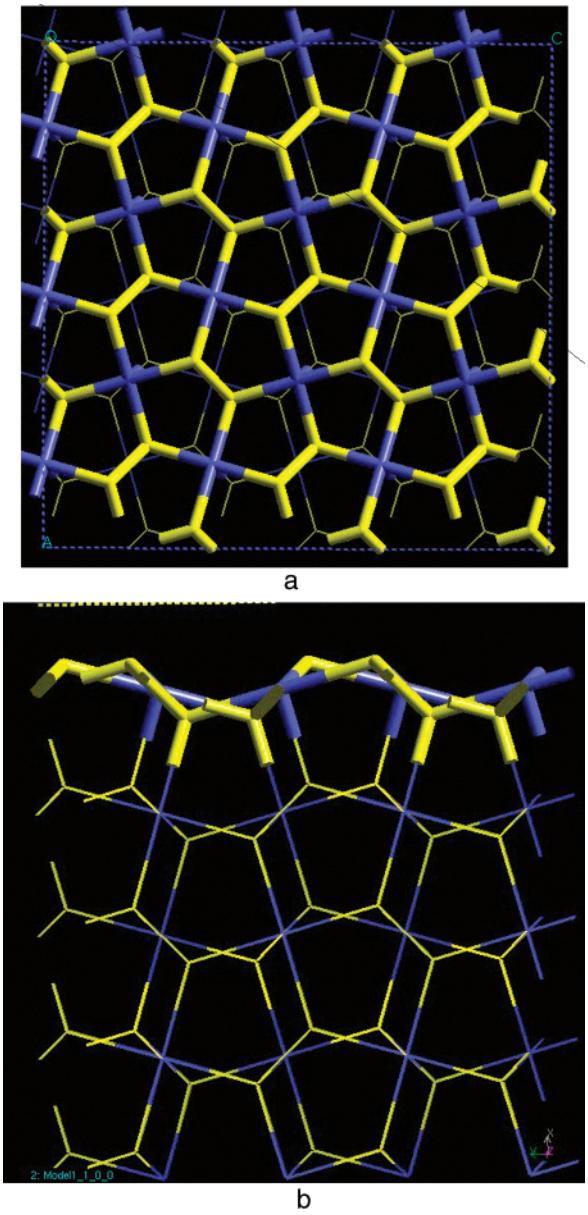

Figure 2. Cylinder model of the (100) surface of RuS_2 showing (a) the top and (b) the side views. Blue and yellow cylinders denote the Ru and S atoms, respectively. Thicker cylinders denote the outermost layer of a unit of S−Ru−S.

The stoichiometric (100) surface exposes the face of the bulk fcc, yielding a two-dimensional (2D) square unit cell (see Figure 2) whose vector length corresponds to the edge of the cube. On each side of a layer of Ru atoms, there is a layer of S atoms. Thus, the stacking of layers can be described as a repetition of S−Ru−S units (see Figure 2a). The S atoms above and below the Ru plane are bonded in inclined S_2 units. The outermost Ru atoms (the second layer) are bonded to five S_2 pairs (SCN = 5). To model a reduced (100) surface, we consider a defect surface with the top S atoms removed. As a consequence, the top Ru atoms are coordinated to only three (SCN = 3) S atoms (see Figure 3).

The (111) surface has a hexagonal unit cell whose vectors lie along the diagonals of the cube faces (Figure 4). This unit cell contains four Ru atoms per layer and eight S atoms above the Ru plane forming four S_2 pairs.[26] Three pairs are tilted on the surface while the remaining one is oriented perpendicular to the surface with one S atom tricoordinated to the closest Ru plane and its topmost sulfur not directly bonded to ruthenium. The S atoms form four layers with slightly different heights on each side of a Ru layer. Thus, there are four S layers between two consecutive Ru layers. Similar to the bulk case, all of the Ru atoms of this surface are hexacoordinated (SCN = 6). The stoichiometric surface[26] is obtained by removing the two outermost S layers (top atoms of the S_2 layers). Then, all of the top S atoms correspond to broken S_2 pairs (see Figure 4c). On the furthest S layer, there are three S atoms in the unit cell, each one sitting on a Ru bridge site, while there is only one on the next S layer, which is located on a 3-fold Ru site. The topmost Ru plane of this surface contains hexa- and pentacoordinated atoms. Hydrogenation of this surface yields exclusively protonic SH groups. Further reduction of one bridge sulfur atom per unit cell leads to a hollow site formed by three pentacoordinated ruthenium (SCN = 5) atoms and one tetracoordinated (SCN = 4) Ru atom (see Figure 5). Hydrogenation of this surface yields to a stable hydrogen overlayer involving

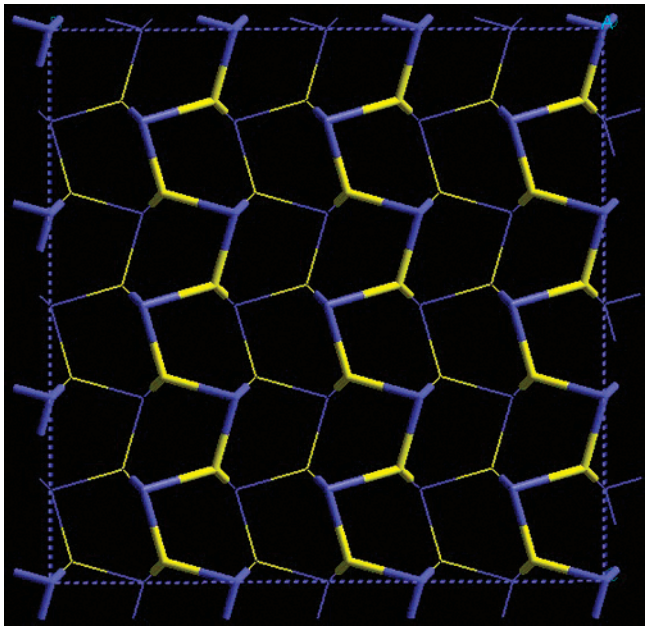

Figure 3. Top view of a cylinder model of a reduced (100) RuS_2 surface. Blue and yellow cylinders denote the Ru and S atoms, respectively. Thicker cylinders show the outermost Ru−S layer.

a hydride species.[27] For this unsaturated surface, a Ru−H bond is formed with the tetracoordinated Ru atom. Thus, its unit cell contains three protonic SH groups (see Figure 6) and a hydridic Ru−H one. To consider the largest range of values in SCN and the effect of the bonded H atoms, we have studied the surfaces of Figures 2, 3, 5, and 6.

The surfaces were modeled by cells containing a periodic slab of several layers of atoms having the structures shown in those figures. In the remainder of the present paper, these surfaces will be called R5, R3, R4, and 4HR4, according to the SCN of the studied Ru atom and the hydrogen coverage. Vacuum layers thicker than 15 Å were used to ensure that there were no interactions between adjacent slabs. The geometry of those models was optimized using the algorithms included in the CASTEP[28] program. In this program, the Kohn−Sham equations of DFT are variationally solved in a plane-wave basis set using optimized ultrasoft pseudo-potentials in Kleinman−Bylander form[29] for the description of the electron−ion interactions. A conjugate gradients minimization scheme is utilized to locate the electronic ground states directly. The generalized gradient approximation of Perdew and Wang[30] is also utilized. The calculation of the Hellmann−Feynman forces acting on the atoms and a standard BFGS technique allows the structural optimization. In agreement with experiment[31] and previous calculations,[32,33] the relaxation obtained for R5 and R3 is negligible leaving to the Ru−S bonds with almost the same value that they have in the bulk[21] (Ru−S bond distance = 2.356 Å). In fact, the study of the reduction process of RuS_2 has shown that near 50% of the sulfur content can be removed from the surface without perceptible structural modification of the surface.[23] In contrast, the higher S layers of R4 undergo a significant contraction resulting in a Ru(tetracoordinate)−S bond length of 2.328, 2.291, and 2.212 Å for the first, second, and third sulfur layers, respectively. Hydrogenation reverts this sulfur relaxation trend, and the corresponding Ru−S lengths in 4HR4 are 2.334, 2.307, and 2.244 Å, respectively. These results are consistent with previous theoretical studies[26,27,32] using Hartree−Fock and DFT methods.

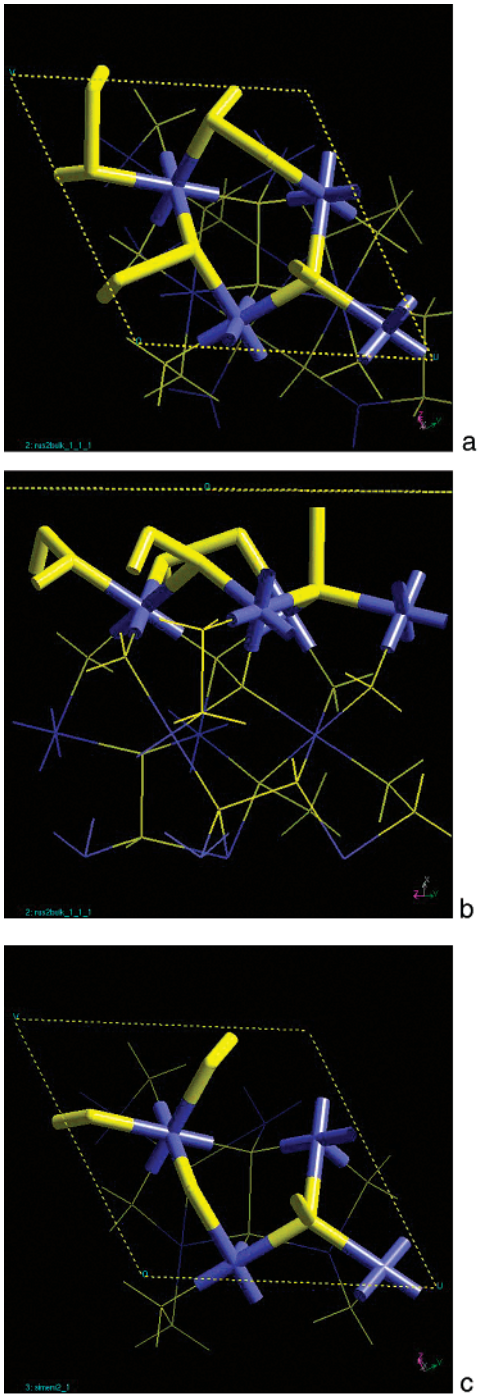

Figure 4. (a) Top view and (b) side view of a cylinder model of the (111) RuS_2 surface unit cell. (c) Top view of the stoichimetric (111) RuS_2 surface. Blue and yellow cylinders denote the Ru and S atoms, respectively. Thicker cylinders show the outermost Ru−S layer.

Computational Methodology

The electron densities for the optimized geometries were calculated by means of the WIEN-97[34] program using a Kohn−Sham Hamiltonian that includes the generalized gradient approximation of Perdew et al.[35] and the spin unrestricted scheme to obtain spin-polarized wave functions. WIEN-97 contains a full potential linearized augmented plane-wave (FLAPW) method[34] that is considered to be among the most accurate methods for performing electronic structure calculations for crystals. The unit cell is divided into a region containing nonoverlapping atomic spheres (centered at the atomic sites) called muffin-tins, MT, and an interstitial region, IT. In the two

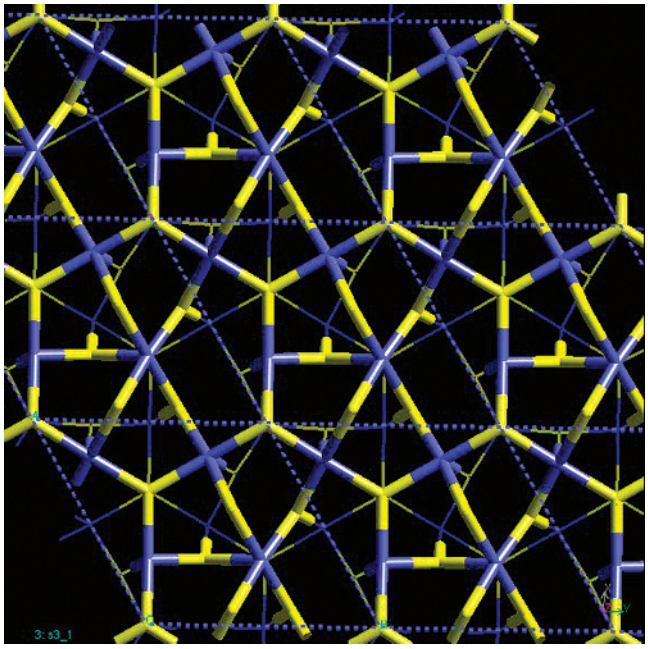

Figure 5. Top view of a cylinder model of the reduce (111) RuS_2 surface containing hollow sites (denotes as an open arrows) created by an S atom bridge vacancy. Blue and yellow cylinders denote the Ru and S atoms, respectively. Thicker cylinders show the outermost layer.

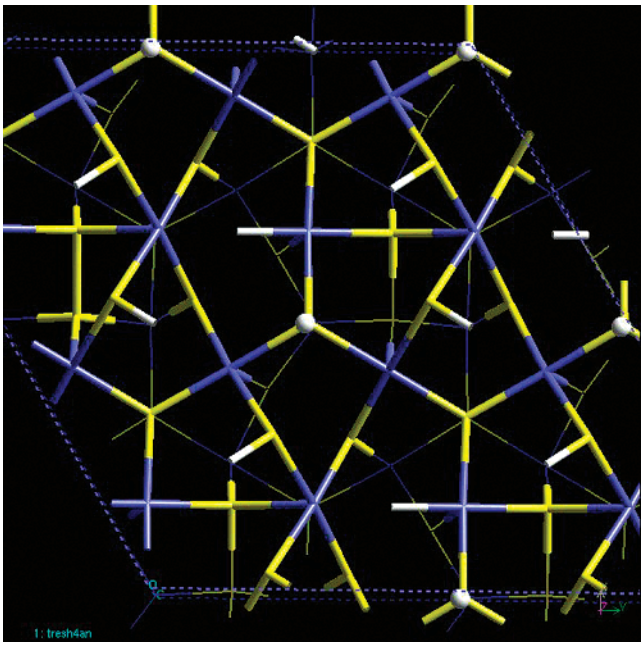

Figure 6. Top view of a cylinder model of the hydrogenated (111) RuS_2 surface. Blue, yellow, and white cylinders denote the Ru, S, and H atoms, respectively.

types of regions, different basis sets are used as follows: a linear combination of radial functions times spherical harmonics inside the atomic sphere and a plane-wave expansion in the IT. Inside the spheres, the potential and charge density were expanded in lattice harmonics up to $l = 12$. A basis set size of about 380 augmented plane-waves per atom with cutoffs $R_{MT}K_{max} = 9.0$ was used. Fifty-six points over the Brillouin Zone and quadratic tetrahedron method were chosen for k-space numerical integration. The topology of $L(\mathbf{r})$ was analyzed using a local version of the BUBBLE program[36] and adapted for the WIEN 97 code in a similar way to the recently reported implementation[37] of the topology of $\rho(\mathbf{r})$.

TABLE 1: Values (Atomic Units; 1 au = 1e/a_0^5) of $L(\mathbf{r})$ at the VSCC CPs of the Topmost Ru Atoms of the (100) and (111) RuS_2 Surfaces

CP type[a]	position[b]	R5	bulk[c]
one F	outer (F^{O}_{Ru})	0.828	0.467
four E	outer	5.375	5.228
four V	outer	6.783	
four F	in along the Ru−S bonds in	0.366	0.467
four E	in along the Ru−S bonds in	4.884	5.228
four V	inner	6.973	
four E	inner	5.311	5.228
one F	along the Ru−S (four layer) bond	0.209	0.467

CP type	position	R3
one F	outer (F^{O}_{Ru})	0.907
four E	outer	5.427
four V	outer	6.458
two F	middle, opposite the top Ru−S (second layer) bond	1.336
two F	middle, along the top Ru−S (second layer) bond	0.440
four E	middle, in the Ru−S (second layer) plane	4.436
four E	inner	5.296
four V	inner	6.602
one F	inner	0.165

CP type	position	R4
one F	outer (F^{OR}_{Ru}), opposite to the hollow	1.641
one F	outer (F^{OL}_{Ru}), toward to the hollow	1.711
one E	outer	5.240
three E	outer, opposite to the hollow	4.838
two V	outermost, bonded to outermost E	5.863
two V	outer, opposite to the hollow	6.385
two E	middle, toward the hollow	4.792
two E	middle, opposite to the hollow	4.724
two F	middle, along the Ru−S bond	1.063
two V	inner, toward the hollow	6.317
two V	inner, bonded to innermost E	6.076
four E	inner	4.734
two F	inner	0.650

CP type	position	4HR4
one F	outer (F^{OR}_{Ru}), opposite to the hollow	1.427
one E	outer	4.246
three E	outer, opposite to the hollow	4.163
two V	outermost, bonded to outermost E	5.238
two V	outer, opposite to the hollow	5.509
four E	middle, toward to the hollow	4.395
one F	middle, toward to the hollow	0.791
three F	middle	0.736
four V	inner	5.574
four E	inner, toward the hollow	4.146
one F	inner	0.189

[a] V, E, and F denote vertex (maximum CP), edges (saddle CP), and face (minimum CP), respectively. [b] The position of the CPs are given with respect to the layer containing the topmost Ru nucleus. [c] Ref 21.

Results

We have located all of the critical points (CPs) on the valence shell charge concentrations, VSCC,[38] of the outermost Ru and S atoms for the studied surfaces. The metal atoms, as in free and bulk atoms,[21] exhibited only four shells of charge concentrations, so that 4s4p4d electrons form the VSCC. The number, positions, and $L(\mathbf{r})$ values at the calculated CPs for the Ru atoms are listed in Table 1. The corresponding atomic graphs, AG, are shown in Figure 7. Similar to the bulk case,[21] the top Ru atoms show a cubelike AG with a set of indices equal to (8, 12, 6), in which eight vertexes are linked by 12 edges and there are six faces joining those vertexes. Each face is defined by

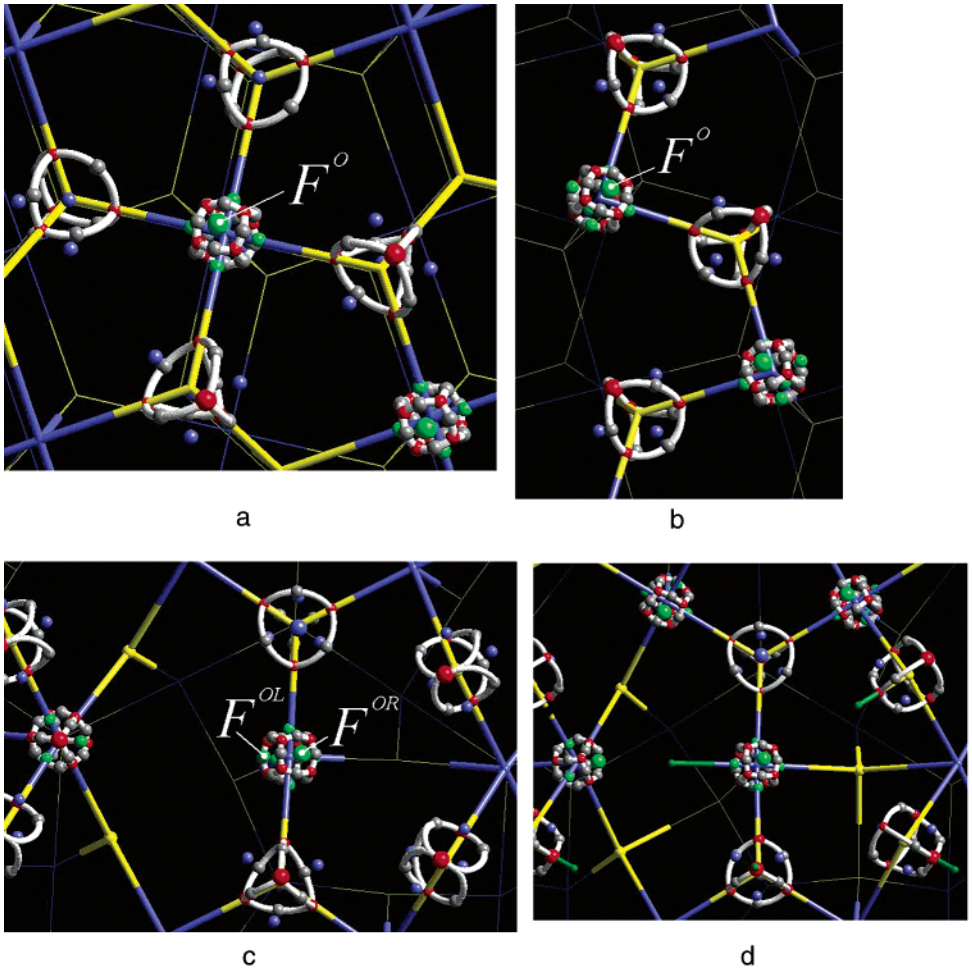

Figure 7. Top view of a model of (a) the (100), (b) the reduced (100), (c) the reduced (111), and (d) the hydrogenated (111) RuS_2 surfaces showing the AGs of the top atoms. Blue, yellow, and green cylinders denote the Ru, S, and H atoms, respectively. Red and gray spheres denote the vertex and edges of the graph, respectively. Green and blue spheres denote the faces CPs of the Ru and S atoms, respectively, and white lines denote the Laplacian gradient trajectories defining the edges of the graphs.

four edges. All of the vertexes are nonbonded local charge concentrations. For R5, the graph (see Figure 7a) exhibits a local minimum, F^{O}_{Ru}, surrounded by four maxima, outside the surface. Additionally, there is a local charge minimum in the middle of each bonded face, pointing toward the five bonded S atoms. Similarly, the top Ru atoms of R3 (see Figure 7b) exhibit a face F^{O}_{Ru} outside the surface and a local charge minimum pointing toward each of the three bonded S atoms. Two of these faces are located along the outermost Ru−S bonds, and opposite to them, there are other two faces placed along the coordination unsaturation. The AG of the S atoms for these surfaces has a tetrahedron-like appearance, characterized by a (4, 6, 4) set of indices with three bonded charge concentration V_S located along the Ru−S bonds. The remaining vertex for the inner S atoms is bonded to a second S atom while it is a nonbonded CP (herein denoted as V_{Snb}) for the outermost S atoms of the surfaces. For R5, these V_{Snb} are located on the first layer of atoms and therefore above F^{O}_{Ru}, while for the R3 case they are located below them. The corresponding graph for the tetracoordinated Ru atoms of the R4 surface shows (see Figure 7c) an edge CP surrounded by two vertexes and two local minima outside the surface. These two minima are located toward and opposite to the hollow site, and they will be denoted as F^{OL}_{Ru} (left to the tetracoordinated Ru) and F^{OR}_{Ru} (right to the tetracoordinated Ru), respectively. The R4 surface has two layers of S atoms above the tetracoordinated Ru atoms. The first S layer contains

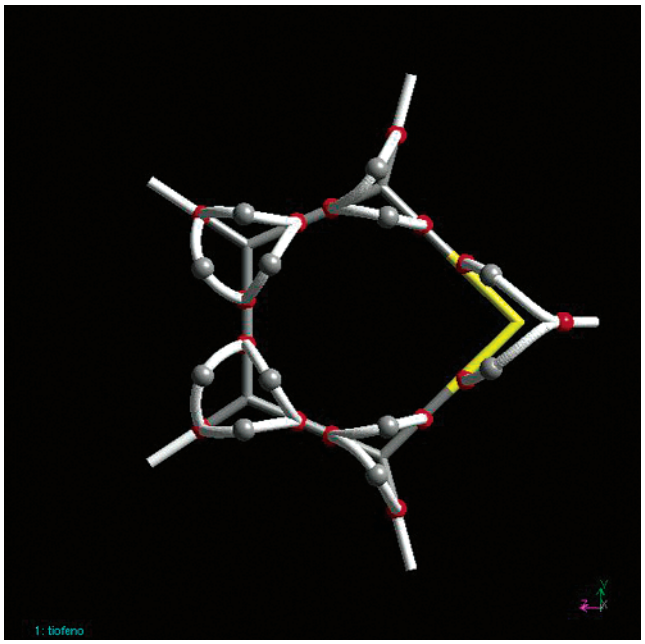

Figure 8. Top view of a model of the TP molecule showing the AGs of the sulfur (yellow cylinder) and carbon (gray cylinders) atoms. Red and gray spheres denote the vertex and edges of the graph, respectively. White lines denote the Laplacian gradient trajectories defining the edges of the graphs.

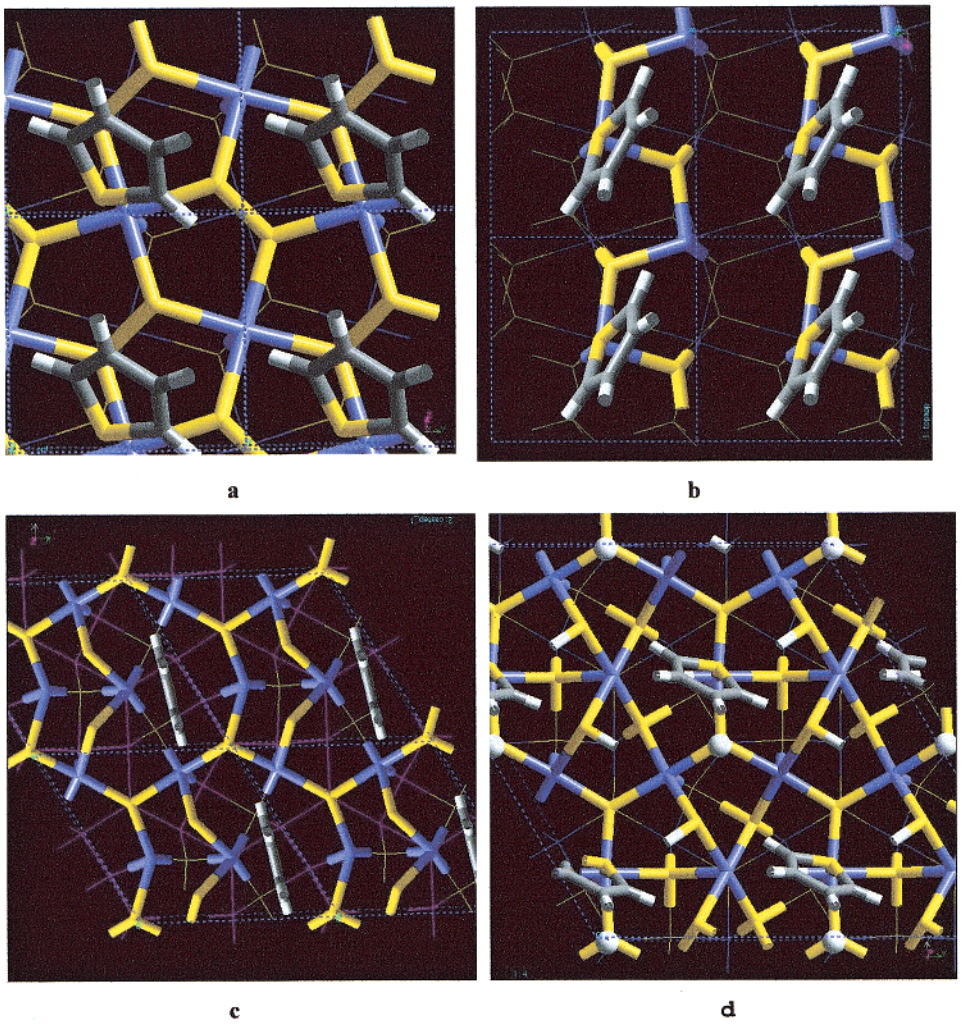

Figure 9. Cylinder model representation of a top view of the equilibrium TP configuration for perpendicular adsorption (η_1) on the (a) (100) surface, (b) reduced (100) surface, (c) (111) surface, and (d) hydrogenated (111) surface of RuS_2. Blue, yellow, and white cylinders denote the Ru, S, and H atoms, respectively.

atoms located in a bridge site on two pentacoordinated Ru atoms. Each of these S atoms possesses a (3, 6, 5) AG, which exposes a nonbonded vertex outside the surface. The S atoms of the second layer are located on a trifold Ru site, and like the R5 and R3 surfaces, they exhibit a tetrahedron-like (4, 6, 4) AG that also shows a V_{Snb} above the surface. It is interesting to note that these V_{Snb} are heaped on the F_{Ru}^{OR} CPs. The AG for 4HR4 is almost identical to the one for the R4 case, except for the localization of F_{Ru}^{OL} along the hydridic Ru−H bond, not present in R4. On the contrary, H coordination to the bridge S atoms produces drastic changes in the sulfur AG. In this graph, a new vertex is formed and a face disappears, such that the AG becomes a tetrahedron-like (4, 6, 4) that exhibits an edge surrounded by two faces outside the surface. Thus, hydrogenation of the R4 surface just clears the space (moving the vertex away) around F_{Ru}^{OR}.

Laplacian topology[38] predicts that the adsorption pathway is initially determined by the mutual alignment of a vertex in the incoming molecule with a face on the top atoms of the surfaces or vice versa. The sulfur atom of the TP molecule has an AG characterized by a (4, 5, 3) set of indices with two bonded maxima along the S−C bonds and two nonbonded maxima above and below the plane of the nuclei (see Figure 8). Each α-C atom has a (3, 4, 3) AG with three bonded vertexes and three faces located at the nuclei plane and four edges located above and below this plane while the β-C atoms show a (3, 6, 5) AG with six edges placed above and below the nuclear plane. These edges CPs represent the largest out-of-plane nonbonded local concentration of electronic charge on the C frame. TP adsorption[21] involves attractive interaction between the vertex on the S atom, $(V_{Snb})_{TP}$, and the edges on the C atoms, E_C, with the faces on the outermost Ru atoms of the surface, F_{Ru}. From Figure 7, it is clear that the AGs on the different surfaces can provide very different environments to the incoming molecules. If the TP adsorption only involves the S atoms of TP and just a Ru atom on the surface, the topology-based theory predicts that the attractive interactions $(V_{Snb})_{TP} \rightarrow F_{Ru}$ will become stronger as the value of $L(\mathbf{r})$ at the face CP decreases. Thus, from Table 1, the trend of TP adsorption strength that we should expect is R5 (0.83 au) > R3 (0.91 au) ≫ 4HR4 (1.43 au) > R4 (1.64 au). We investigated binding of TP in the η_1 adsorption configuration (i.e., for the molecule with the ring perpendicular to the surface) on the considered sites, using DFT calculations with CASTEP. A TP molecule was placed inside the surface unit cell, on the considered Ru atom, aligned as the $L(\mathbf{r})$ topology predicts. The geometry was fully optimized to their most energetically favorable positions, maintaining fixed the two innermost layers at the bottom of the cell. The predicted geometries are shown in Figure 9. For R5, R3, and 4HR4, the TP molecule adopts a η_1 tilted position, while for R4 it prefers to be located at the hollow site in a bridge position. The trend of binding energy, BE, obtained was 4HR4 (0.78 eV) > R3

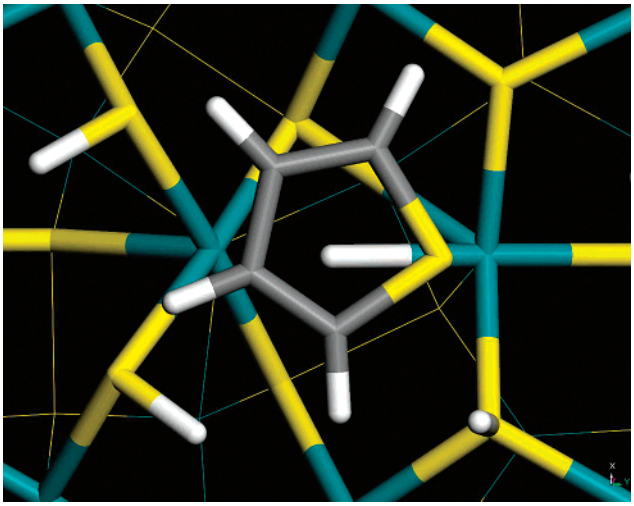

Figure 10. Cylinder model representation of a top view of the equilibrium TP configuration for perpendicular adsorption (η_5) on the hydrogenated (111) surface of RuS_2. Blue, yellow, and white cylinders denote the Ru, S, and H atoms, respectively.

(0.50 eV) > R4 (0.44 eV) ≅ R5 (0.43 eV). From this trend, it is evident that in the adsorption of TP on the RuS_2 surfaces other additional interactions different from $(V_{Snb})_{TP} \rightarrow F_{Ru}$ should be considered. Inspection of Figures 7−9 show that TP binds at the surface moving away from the V_{Snb} closest to the Ru atoms, minimizing the repulsive interactions $(E_C)_{TP} \leftrightarrow (V_{Snb})_{surface}$. Thus, despite the fact that $L(F_{Ru})_{R3} > L(F_{Ru})_{R5}$, the smallest repulsion $E_C-(V_{Snb})_{surface}$ caused by the loss of the outermost S layer in R3 with respect R5 leads to a bigger binding energy for TP. In the case of R4, the nonbonded vertexes of the top sulfur atoms form a real shield around F^{OR}_{Ru} obstructing its interaction with the vertex of the incoming TP, pushing the molecule to a bridge coordination. It is important to emphasize that despite the big $L(F_{Ru})$ value for R4, the interaction of TP ($F_{Ru} \leftarrow (V_{Snb})_{TP} \cdots (V_{Snb})_{TP} \rightarrow F_{Ru}$) toward two atoms of the surface leads to a BE value similar to the corresponding value on R5 and R3. Finally, the results also show that only surface hydrogenation leads to an appreciable increment of the adsorption strength of TP. In this sense, Laplacian topology shows that the formation of the S−H bonds moves the $(V_{Snb})_{surface}$ away from F^{OR}_{Ru} favoring the attractive interaction $(V_{Snb})_{TP} \rightarrow F^{OR}_{Ru}$.

In agreement with previous studies,[24,33] there is no sign of TP activation (no changes of the TP bonds) on the η_1 adsorption (the most stable adsorption geometry) over the R5, R3, and R4 models. This activation was just observed[24] for a parallel orientation of the TP ring with respect to the 4HR4 surface plane with the ring centered over the hydride species. We have also studied this parallel adsorption geometry, and the result is shown in Figure 10. The computed highest adsorption energy (1.20 eV) corresponds to a $\eta_{parallel}$ bonding mode involving the attractive interactions $F_{Ru} \leftarrow (E_{C\beta})_{TP}$, $(V_{Snb})_{TP} \rightarrow F_{Ru}$, and $H^- \rightarrow F_{C\alpha}$ toward the five- and four-coordinated Ru atoms located at the left and the right of the hollow sites and to the C_α face at the plane of the TP molecule, respectively. On this geometry, the attractive interactions of C_β and S atoms of TP toward two different Ru atoms on the surface, as well as the retro-attack of the surface hydride to the C_α of the TP molecule, ultimately must to lead to C−S bond scission and sulfur removal.

The present results corroborate the idea that the largest tendency to C−S bond activation is obtained on a coordinative unsaturated Ru−H site and confirm the experimental[23] relationships between the concentration of hydridic species chemisorbed on coordinatively unsaturated Ru cations and the hydrogenation catalytic activity for unsupported ruthenium−sulfide catalyst. Additionally, our results also show that low sulfur coordination of the ruthenium cations does not necessarily increase the Ru-based catalyst activity. Low sulfur coordination increases the value of the Laplacian at the Ru-exhibited faces so the strength of their interaction with the S atom of TP decreases. This finding agrees and explains the experimentally[39] observed decrease of the pyridine adsorption on RuS_2 catalyst at severe reduction conditions.

Summary

The AG of the most external atoms in the surfaces can provide very different environments to the incoming molecules. Nevertheless, the Ru atoms of these surfaces exhibit the same type of AG that the atoms of the bulk, regardless of how many sulfur atoms they are coordinated to. Consequently, surfaces and bulk show the same kind of interaction between the Ru and the S atoms. If the adsorption only involved the S atom of TP and just a Ru atom on the surface, the interaction $(V_{Snb})_{TP} \rightarrow F_{Ru}$ will be stronger as the value of $L(\mathbf{r})$ at the face CP decreases. However, this interaction is strongly affected by the presence of the surface sulfur vertexes. A maximum SCN to Ru leads to the smallest value of $L(F_{Ru})$, favoring the attractive $(V_{Snb})_{TP} \rightarrow F_{Ru}$. Nevertheless, it also increases the number of $(V_{Snb})_{surface}$ CPs in the Ru neighborhood increasing the repulsive interaction between $(V_{Snb})_{TP}$ and E_Cs with the vertexes of the outermost surface S atoms. Both factors combine in such way that the strength of the TP adsorption in the favorite configurations (h_1 on a single atom of Ru for R5 and R3 and a bridge on two atoms of Ru for R4) on the unhydrogenated surfaces only shows small changes. In this aspect, the main role of the protonic hydrogen atoms consists of moving away from the Ru surroundings, the vertexes that impede its interaction with the TP molecule. On the hydrogenated surface studied in this work, TP prefers to adsorb in $\eta_{parallel}$ (TP molecular plane oriented parallel to the surface) modes in which the interaction of a hydride species with a local minimum located at the C_α of TP mainly leads to the C−S bond breaks.

Acknowledgment. This work was supported by Grant G-2000001512 from the CONICIT (Consejo Nacional de Investigaciones Científicas y tecnológicas) of Venezuela.

Appendix

Laplacian of the Electronic Charge Density. From a quantum chemical point of view, $L(\mathbf{r})$ constitutes one of the most powerful tools for extracting the chemical information[38,40] contained in the charge density of molecular systems and materials, and in addition, it is particularly important for the purpose of understanding chemical reactivity and molecular interactions. This topological approach has the advantage of allowing scientists to directly explore the interaction of molecules on surfaces in terms of the properties of $\rho(\mathbf{r})$.

In general, the atomic Laplacian[38] evinces alternating shells of charge concentration and depletion equal in number to the number of quantum shells. The outer VSCC contains a surface, S_{VSCC}, over which ρ is maximally concentrated. The distribution of $L(\mathbf{r})$ over this surface is uniform for a free atom. Although S_{VSCC} persists when the atom is in chemical combination, it no longer evinces a uniform concentration. The formation of a bond alters this surface charge distribution, and a number of CPs (local maxima, minima, and saddle points) appear on S_{VSCC}.[38] The localized concentrations of charge mimic the pairs of electron

assumed in the Lewis model in number, relative positions, and sizes.[38,40] The radial curvature, that is, the curvature of $L(\mathbf{r})$ normal to S_{VSCC}, is negative. On the other hand, the two tangential curvatures can assume either positive or negative values. If both of these curvatures are negative or positive, then a local maximum or local a minimum is formed, respectively, on the surface. When one of the tangential curvatures is negative and the other positive, a saddle is formed. Each maximum[38,40] is linked to another one by a unique pair of trajectories, i.e, vector paths defined by the gradient of $L(\mathbf{r})$, which originate at the saddle points. The network of these trajectories partitions S_{VSCC} into segments having curved faces. At the center of each of these faces belonging to the VSCC surface, there is a local minimum. This structure is called an AG[38] and succinctly summarizes the types and the numbers of CPs formed on the VSCC of an atom in a molecule. This graph provides the connectivity of the extremes of $L(\mathbf{r})$ in the corresponding surface of charge concentration of the VSCC distribution. The AG is most easily visualized in terms of a polyhedron whose vertexes (V), edges (E), and faces (F) satisfy Euler's formula:[38]

$$n_V - n_E + n_F = 2$$

The local maxima define the vertexes. The unique pair of trajectories, which originate at the saddle CPs, define the edges, and the local minima define the faces. These graphs can be easily classified in terms of the (n_V, n_E, n_F) indices, which are the numbers of vertexes, edges, and faces, respectively. Making use of these graphs, a general Lewis acid−base reaction, customarily described in terms of aligning the charge concentrations of the VSCC on the base with the charge depletion on the acid, may be alternatively described by directing a vertex of the graph for the base atom toward the face of the polyhedron for the acid. Laplacian topology predicts that the adsorption pathway of a molecule on a surface is determined by mutual alignment of a vertex in the incoming molecule with a face on the top atoms of the surface or vice versa.[21,41]

References and Notes

(1) Weisser, O.; Landa, S. *Sulfide Catalysts: Their Properties and Applications*; Pergamon: Oxford, 1973.

(2) Topsoe, H.; Clausen, B. S.; Massoth, F. *Hydrotreating Catalysis in Catalysis, Science and Technology*; Springer-Verlag: Berlin, 1996; Vol. 11.

(3) Rodriguez, J. A.; Drovak, J.; Capitano, A. T.; Gabelnick, A. M.; Gland, J. L. *Surf. Sci.* **1999**, *429*, L462.

(4) Pecoraro, T. A.; Chianelli, R. R. *J. Catal.* **1981**, *67*, 430.

(5) Chianelli, R. R.; Daage, M.; Ledoux, M. J. *Adv. Catal.* **1994**, *40*, 117.

(6) Harris, S.; Chianelli, R. R. *J. Catal.* **1984**, *86*, 400.

(7) Topsoe, H.; et al. *Bull Soc. Chim. Belg.* **1995**, *104*, 283.

(8) Norskov, J. K.; Clausen, B. S.; Topsoe, H. *Catal. Lett.* **1992**, *1*, 13.

(9) Vissers, J. P. R.; Groot, C. K.; van Oers, E. M.; J. de Beer, V. H.; Prins, R. *Bull. Soc. Chim. Belg.* **1984**, *93*, 813.

(10) Ledoux, M. J.; Michaux, O.; Agostini, G.; Panissod, P. *J. Catal.* **1986**, *102*, 275.

(11) Burdett, J. K.; Chung, J. T. *Surf. Sci. Lett.* **1990**, *236*, L353.

(12) Smit, T. S.; Johnson, K. H. *Catal. Lett.* **1994**, *28*, 361.

(13) Raybaud, P.; Kresse, G.; Hafner, J.; Toulhoat, H. *J. Phys.: Condens. Matter* **1997**, *9*, 11085.

(14) Raybaud, P.; Kresse, G.; Hafner, J.; Toulhoat, H. *J. Phys.: Condens. Matter* **1997**, *9*, 11107.

(15) Raybaud, P.; Hafner, J.; Kresse, G.; Toulhoat, H. *Phys. Rev. Lett.* **1998**, *80*, 1481.

(16) Raybaud, P.; Hafner, J.; Kresse, G.; Toulhoat, H. *Surf. Sci.* **1998**, *407*, 237.

(17) Toulhoat, H.; Raybaud, P.; Kasztelan, S.; Kresse, G.; Hafner, J. *Catal. Today* **1999**, *50*, 629.

(18) Raybaud, P.; Hafner, J.; Kresse, G.; SKasztelan, S.; Toulhoat, H. *J. Catal.* **2000**, *190*, 128.

(19) van Santen, R. A.; Neurock, M. *J. Am. Chem. Soc.* **1994**, *116*, 4427.

(20) Aray, Y.; Rodriguez, J.; Vega, D.; Rodriguez-Arias, E. N. *Angew. Chem. Int. Ed.* **2000**, *39*, 3810.

(21) Aray, Y.; Rodríguez, J. *ChemPhysChem* **2001**, *10*, 599.

(22) Hensen, E. J. M.; Brans, H. J. A.; Lardinois, G. M. H. J.; de Beer, V. H. J.; van Veen, J. A. R.; van Santen, R. A. *J. Catal.* **2000**, *192*, 98.

(23) (a) Jobic, H.; Clugnet, G.; Lacroix, M.; Yuan, S.; Mirodatos, C.; Breysse, M. *J. Am. Chem. Soc.* **1993**, *115*, 3654. (b) Lacroix, M.; Yuan, S.; Breysse, M.; Doremieux-Morin, C.; Fraissard, J. *J. Catal.* **1992**, *138*, 409. (c) Breysse, M.; Geantet, C.; Lacroix, M.; Portefaix, J.-L.; Vrinat, M. In *Hydrotreating Technology for Pollution Control*; Occelli, M. L., Chianelli, R., Eds.; Marcel Dekker: New York, 1999.

(24) Grillo, M. E.; Sautet, P. *J. Mol. Catal. A* **2001**, *3195*, 1.

(25) Lutz, H. D.; Mueller, B.; Schimidt, T.; Sting, T. *Acta Crystallogr., Sect C* **1990**, *46*, 2003.

(26) Grillo, M. E.; Smelyansky, V.; Sautet, P.; Hafner, J. *Surf. Sci.* **1999**, *439*, 163.

(27) Grillo, M. E.; Sautet, P. *Surf. Sci.* **2000**, *457*, 285.

(28) CASTEP Release; Accelerys Inc.: San Diego, CA.

(29) Kleinman, L.; Bylander, D. M. *Phys. Rev. Lett.* **1982**, *48*, 1425.

(30) Perdew, J. P.; Wang, Y. *Phys. Rev.* **1992**, *B45*, 13244.

(31) Collel, H.; Bronold, M.; Fletcher, S.; Tributsch, H. *Surf. Sci.* **1994**, *303*, L361.

(32) Frechard, F.; Sautet, P. *Surf. Sci.* **1995**, *336*, 149.

(33) Smelyansky, V.; Hafner, J.; Kresse, G. *Phys. Rev. B* **1998**, *58*, 1782.

(34) Blaha, P.; Schwarz, K.; Luitz, J. *WIEN 97*; Vienna University of Technology: Vienna, 1997. (Improved and updated Unix version of the original copyrighted WIEN-code, which was published by Blaha, P.; Schwarz, K.; Sorantin, P.; Trickey, S. B. *Comput. Phys. Commun.* **1990**, *59*, 399.)

(35) Perdew, J. P.; Burke, S.; Ernzerhof, M. *Phys. Rev. Lett.* **1996**, *77*, 3865.

(36) Bader, R. F. W.; Krugg, P. *AIMPAC*; Department of Chemistry, McMaster University: Hamilton, Ontario, Canada, 1990 (http://www.chemistry.mcmaster.ca/aimpac/).

(37) Aray, Y.; Rodríguez, J.; Vega, D. *Comput. Phys. Commun.* **2002**, *143*, 199.

(38) (a) MacDougall, P. J. The Laplacian of the Electronic Charge Density. Ph.D. Thesis, McMaster University, Canada, 1989. (b) Bader, R. F. W. *Atoms in Molecules—A Quantum Theory*; Claredon: Oxford, U.K., 1990. (c) Popelier, P. *Atoms in Molecules—An Introduction*; Prentice Hall: U.K., 2000.

(39) Berhault, G.; Lacroix, M.; Breysse, M.; Mauge, F.; Lavalley, J.-C.; Nie, H.; Qu, L. *J. Catal.* **1998**, *178*, 555.

(40) (a) MacDougall, P. J.; Hall, M. B. *Trans. Am. Crystallogr. Assoc.* **1990**, *26*, 105. (b) Bader, R. F. W.; MacDougall, P. J.; Lau, C. D. *J. Am. Chem. Soc.* **1984**, *106*, 1594. (c) Bader, R. F. W.; MacDougall, P. J. *J. Am. Chem. Soc.* **1985**, *107*, 6788. (d) Bader, R. F. W.; Popelie, P. L. A.; Chang, C. J. *Mol. Struct. THEOCHEM* **1992**, *255*, 145.

(41) (a) Aray, Y.; Rodriguez, J. *Surf. Sci. Lett.* **1998**, *405*, L532. (b) Aray, Y.; Rodriguez, J.; Rivero, J.; Vega, D. *Surf. Sci.* **1999**, *441*, 344. (c) Aray, Y.; Rodriguez, J.; Vega, D. *J. Phys. Chem. B* **2000**, *104*, 5225.